Journal of Physics Research and Education, Volume 3, March 2026

AI-Enhanced Cascaded Fiber-Optic Sensing Architecture for High-Accuracy Multi-Parameter Monitoring

Koustav Dey
Department of Electrical and Computer Engineering,
Missouri University of Science and Technology, Rolla, MO 65409, USA and
Department of Physics, National Institute of Technology Warangal, TS 506004, INDIA

Nikhil Vangety, Anirban Majee, and Sourabh Roy*
Department of Physics, National Institute of Technology Warangal, TS 506004, INDIA

This work presents a novel approach for the simultaneous measurement of temperature and strain using a cascaded multi–single–multi (MSM) mode fiber structure integrated with an artificial neural network (ANN). Experimental data were systematically acquired to construct a comprehensive dataset for ANN training and validation. The proposed model demonstrates substantial performance improvement, achieving reductions in root mean squared error (RMSE) by factors of 1290 and 303 for temperature and strain estimation, respectively, compared to the conventional transfer matrix method. In addition, the proposed framework provides enhanced sensitivity. These results highlight the potential of the ANN-assisted MSM configuration for high-accuracy multiparameter sensing applications.

I. INTRODUCTION

Over the past two decades, fiber-optic sensors have advanced significantly in sensitivity and resolution due to their inherent advantages [1–3]. Structures such as FBGs [1, 2], LPGs [3], Fabry–Perot interferometers [4–6], and in-fiber interferometers [7, 8] have been widely employed for temperature and strain sensing. However, these configurations often require complex fabrication and costly instrumentation. Although tapering and chemical etching can enhance sensitivity [9, 10], they may reduce mechanical robustness. Multi–single–multi structures, based on modal interference, offer a simple and cost-effective alternative with improved intrinsic sensitivity and favorable spectral characteristics compared to SMS configurations [11–13]. Despite their potential, MSM-based multiparameter sensing remains relatively underexplored [14–16]. Conventional simultaneous temperature–strain measurement relies on peak tracking and the transfer matrix method [7, 8], which suffers from nonlinear coefficient variation and cross-sensitivity issues [17]. To overcome these limitations, artificial neural networks (ANNs) have been increasingly applied in photonic sensing due to their ability to model complex nonlinear relationships [17–21].

In this work, an experimentally fabricated MSM fiber segment is integrated with a trained ANN model for concurrent temperature and strain estimation. The proposed approach demonstrates improved accuracy and performance over traditional analytical methods, highlighting its suitability for multiparameter sensing applications.

* sroy@nitw.ac.in

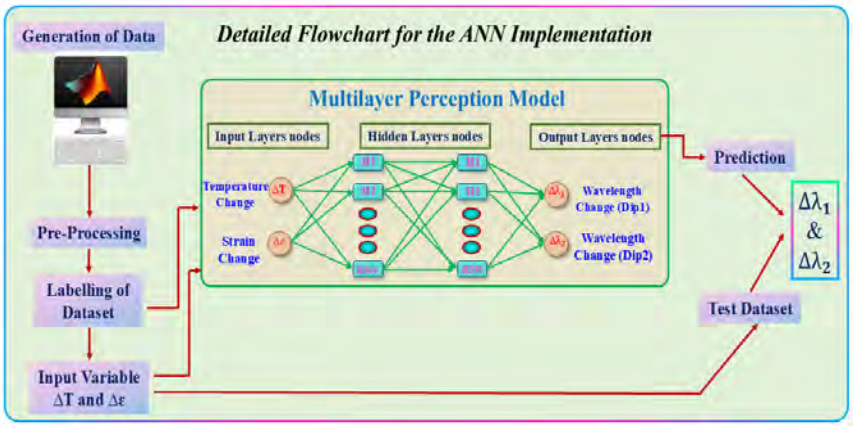

FIG. 1. Detail flowchart and outlayer of the ANN implementation.

II. ARTIFICIAL NEURAL NETWORK–BASED MODELING FRAMEWORK

An artificial neural network is employed to model the nonlinear relationship between the sensing parameters and the spectral response of the MSM structure. Owing to its capability to learn complex and noisy datasets, the ANN effectively captures inherent nonlinearities and cross-sensitivity effects. The proposed framework, illustrated in Fig. 1, utilizes temperature variation (ΔT) and strain variation ($\Delta\varepsilon$) as input features, while the wavelength shifts of two selected MSM interference dips ($\Delta\lambda_1$ and $\Delta\lambda_2$) serve as output responses. A total of 10,000 data samples were generated through MATLAB-based simulations and used to construct the dataset. These were divided into 90% for training (9,000 samples) and 10% for testing (1,000 samples) to evaluate model performance. A multilayer perceptron (MLP) architecture was adopted for regression analysis. Prior to training, the dataset was normalized and randomly shuffled to eliminate bias and ensure robust generalization.

III. RESULTS AND DATASET ACQUISITION PROCEDURE

The wavelength shifts of the selected interference dips are monitored under the simultaneous influence of temperature and strain perturbations. Due to the inherently nonlinear response of the sensor to these parameters, significant percentage errors may arise if conventional analytical approaches are applied. Such nonlinear cross-dependencies cannot be ignored, as they degrade measurement accuracy. To address this limitation, an ANN-based framework is implemented to effectively model the nonlinear behavior and decouple the sensing parameters, thereby enabling accurate retrieval of temperature and strain with minimal estimation error. This section systematically presents and analyzes these aspects. To construct the transfer matrix formulation, the sensitivity coefficients must first be determined. This is achieved by plotting the wavelength shifts of the two selected spectral dips against variations in temperature and strain. The coefficients are then extracted from the linear fitting of these responses, as illustrated in Fig. 2. Figures 2(a) and 2(b) illustrate the spectral response of the two selected MSM interference dips under temperature and strain perturbations, respectively. A monotonic wavelength shift is observed in both cases. Over the temperature range of 20–100 °C, dip_1 and dip_2 exhibit maximum red shifts of

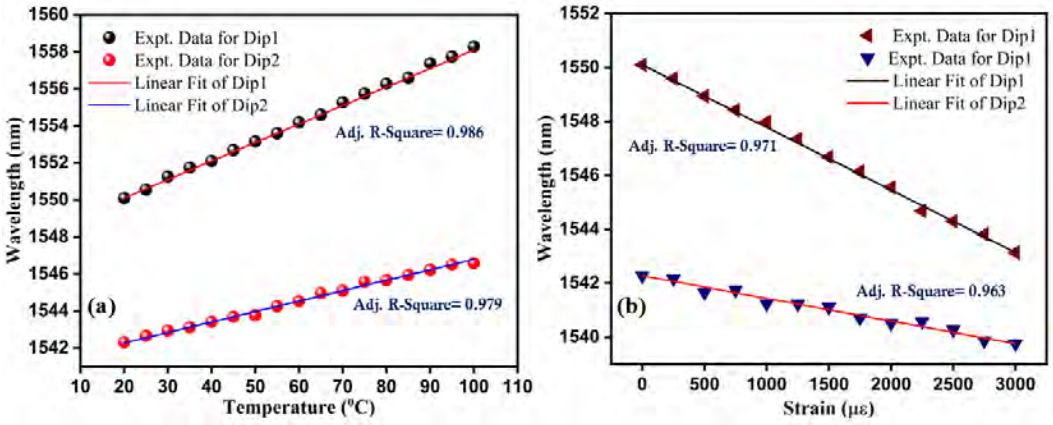

FIG. 2. Wavelength shifts of the two selected interference dips as a function of (a) temperature variation and (b) applied strain.

approximately 8 nm and 4.5 nm, corresponding to sensitivities of $\sim$ 105 pm/°C and $\sim$ 42 pm/°C, respectively. This behavior arises from temperature-induced variations in the effective refractive index and physical dimensions of the SMF section, along with contributions from the thermo-optic effect, collectively shifting the dips toward longer wavelengths. Under applied strain (0–3000 $\mu\varepsilon$), both dips exhibit a blue shift, with maximum wavelength changes of $\sim$ 7 nm (dip_1) and $\sim$ 2.5 nm (dip_2). The corresponding strain sensitivities are $\sim$ 3.22 pm/$\mu\varepsilon$ and $\sim$ 0.60 pm/$\mu\varepsilon$, respectively. The blue shift is attributed to strain-induced changes in the effective refractive index contrast within the SMF segment, which shift the resonance dips toward shorter wavelengths.

Following the experimental analysis, a comprehensive dataset was generated in MATLAB by applying the inverse transfer matrix formulation over the experimentally defined temperature (20–100 °C) and strain (0–3000 $\mu\varepsilon$) ranges, with fine step increments. A total of 10,000 samples were produced, of which 90% (9,000 data points) were used for training and the remaining 10% (1,000 data points) for testing the ANN model. The input dataset consisted of paired temperature (ΔT) and strain ($\Delta\varepsilon$) values, while the corresponding output targets were the wavelength shifts of the two selected dips ($\Delta\lambda_1$ and $\Delta\lambda_2$), enabling effective supervised training of the model. The test dataset was first input into the trained ANN model to evaluate its predictive performance. The resulting wavelength shifts of the two interference dips with respect to temperature and strain are presented in Fig. 3. Figure 3(a) shows a monotonic red shift of both dips with increasing temperature, whereas Fig. 3(b) demonstrates a blue shift under applied strain. These trends are consistent with the expected physical response of the MSM structure. The generated new matrix using the model is

$$\begin{pmatrix} \Delta T \\ \Delta\varepsilon \end{pmatrix} = \frac{1}{88.11} \begin{pmatrix} -0.69\ \text{pm}/\mu\varepsilon & 3.46\ \text{pm}/\mu\varepsilon \\ -48\ \text{pm}/^{\circ}\text{C} & 113\ \text{pm}/^{\circ}\text{C} \end{pmatrix} \begin{pmatrix} \Delta\lambda_1 \\ \Delta\lambda_2 \end{pmatrix}. \tag{1}$$

Using the proposed ANN-based framework, the achieved sensitivities are 3.46 pm/$\mu\varepsilon$ for strain and 113 pm/°C for temperature. The input dataset was generated via MATLAB simulations rather than directly from raw experimental measurements, thereby improving consistency and linearity of the training data. This enhanced dataset coherence contributes to the observed improvement in sensitivity. Moreover, the higher determinant value of the transfer matrix indicates reduced cross-

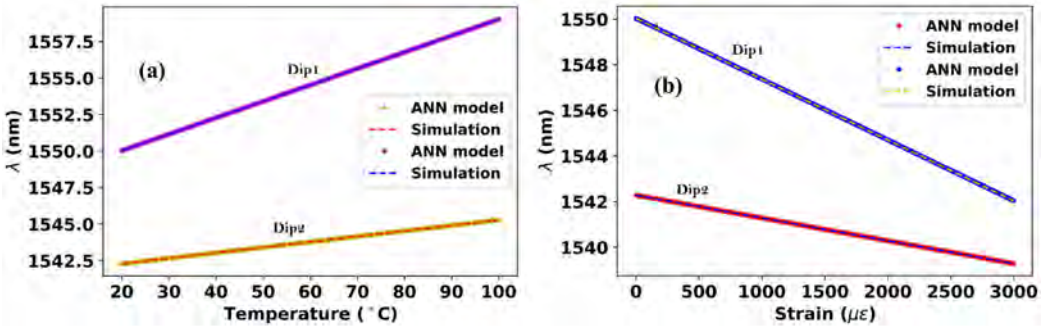

FIG. 3. Comparison of ANN-predicted and simulated wavelength shifts of the two selected dips as a function of (a) temperature and (b) applied strain.

sensitivity between parameters. The model achieves low RMSE values of 0.146 $\mu\varepsilon$ for strain and 0.017 °C for temperature estimation. Notably, the ANN-assisted approach improves accuracy by factors of approximately 1294 and 301 for temperature and strain, respectively, compared to the conventional matrix method.

IV. CONCLUSIONS AND FUTURE PERSPECTIVES

In this work, an AI-enhanced cascaded MSM fiber-optic sensing architecture has been demonstrated for high-accuracy simultaneous temperature and strain monitoring. The proposed approach integrates a cascaded MSM fiber structure with a multilayer perceptron-based artificial neural network to effectively model nonlinear sensor responses and mitigate cross-sensitivity effects. Compared to the conventional transfer matrix method, the ANN-assisted framework significantly improves performance, achieving RMSE reductions by factors of 1290 and 303 for temperature and strain estimation, respectively. The obtained sensitivities of 113 pm/°C and 3.46 pm/$\mu\varepsilon$ further confirm the enhanced sensing capability of the proposed architecture. The improved determinant value of the generated matrix and the low estimation errors demonstrate the robustness of the AI-based decoupling strategy. The results validate that data-driven modeling can overcome limitations associated with nonlinear coefficient variation in traditional analytical approaches.

From a broader perspective, the presented AI-assisted MSM sensing platform can be extended to multi-parameter monitoring beyond temperature and strain, including refractive index, pressure, or biochemical sensing applications. Future work will focus on incorporating real-time experimental datasets for adaptive learning, exploring deep learning architectures to further enhance accuracy, and implementing hardware-level integration for field-deployable smart sensing systems. The proposed framework thus opens a promising pathway toward intelligent, high-precision fiber-optic sensing for industrial and structural health monitoring, as well as advanced photonic applications.

[1] D. P. Zhou *et al.* Appl. Opt. **47**, 1668 (2008).

[2] L. Xiong *et al.*, Chin. Opt. Lett. **12**, 120605 (2014).
[3] A. Iadicicco *et al.*, IEEE Photonics Technology Letters **29**, 1533 (2017).
[4] Q. Liu *et al.*, IEEE Photon. Technol. Lett. **26**, 1715 (2014).
[5] X. Yu, N. Song, and J. Song, Opt. Commun. **459**, 125020 (2020).
[6] J. Tian *et al.*, Opt. Commun. **412**, 121 (2018).
[7] Z. Kang *et al.*, Appl. Opt. **53**, 2691 (2014).
[8] G. Zhang *et al.*, Optik **254**, 168636 (2022).
[9] K. Dey, R. Buddu, and S. Roy, Silicon **14**, 4349 (2022).
[10] S. Sridevi *et al.*, Opt. Lett. **41**, 2604 (2016).
[11] K. Dey *et al.*, Results in Optics **2**, 100039 (2021).
[12] K. Dey and S. Roy, Infrared Physics & Technology **127**, 104356 (2022).
[13] K. Dey and S. Roy, Physica Scripta **97**, 125507 (2022).
[14] Y. Ma *et al.*, IEEE Photonics Technology Letters **32**, 1117 (2020).
[15] B. Yin *et al.*, Optics and Laser Technology **80**, 16 (2016).
[16] Z. Akbarpour, V. Ahmadi, and F. Roghabadi, Opt. Fiber Technol. **73**, 103035 (2022).
[17] K. Dey *et al.*, Opt. Quant. Electron. **55**, 16 (2023).
[18] K. Dey, V. Nikhil, and S. Roy, Sens. Actuators A: Phys. **333**, 113254 (2022).
[19] S. Chugh *et al.* Opt. Express **27**, 36414 (2019).
[20] F.O. Barino and A.B. Santos, IEEE Sensors Journal **20**, 4187 (2020).
[21] G.C. Kahandawa *et al.*, Sensors and Actuators A: Physical **194**, (2013).